Effect of a Y265F Mutant on the Transamination-Based Cycloserine Inactivation of Alanine Racemase[†,‡]

Timothy D. Fenn,[§,||] Todd Holyoak,[§,⊗] Geoffrey F. Stamper,[§,⊥] and Dagmar Ringe*[,§]

Rosenstiel Basic Medical Sciences Research Center, Program in Biochemistry, and Program in Biophysics, Brandeis University, Waltham, Massachusetts 02454

Received October 7, 2004; Revised Manuscript Received January 4, 2005

ABSTRACT: The requirement for D-alanine in the peptidoglycan layer of bacterial cell walls is fulfilled in part by alanine racemase (EC 5.1.1.1), a pyridoxal 5′-phosphate (PLP)-assisted enzyme. The enzyme utilizes two antiparallel bases focused at the C_α position and oriented perpendicular to the PLP ring to facilitate the equilibration of alanine enantiomers. Understanding how this two-base system is utilized and controlled to yield reaction specificity is therefore a potential means for designing antibiotics. Cycloserine is a known alanine racemase suicide substrate, although its mechanism of inactivation is based on transaminase chemistry. Here we characterize the effects of a Y265F mutant (Tyr265 acts as the catalytic base in the L-isomer case) of *Bacillus stearothermophilus* alanine racemase on cycloserine inactivation. The Y265F mutant reduces racemization activity 1600-fold [Watanabe, A., Yoshimura, T., Mikami, B., and Esaki, N. (1999) *J. Biochem. 126*, 781−786] and only leads to formation of the isoxazole end product (the result of the transaminase pathway) in the case of D-cycloserine, in contrast to results obtained using the wild-type enzyme. L-Cycloserine, on the other hand, utilizes a number of alternative pathways in the absence of Y265, emphasizing the importance of Y265 in both the inactivation and racemization pathway. In combination with the kinetics of inactivation, these results suggest roles for each of the two catalytic bases in racemization and inactivation, as well as the importance of Y265 in "steering" the chemistry to favor one pathway over another.

D-Amino acids tend to be concentrated in bacterial cell walls and the nervous system of mammals (*2*−*4*). In the former case, D-alanine and D-glutamate form an integral part of the oligopeptide linker in the peptidoglycan layer (*4*). While D-glutamate is generated either via chiral reduction of α-ketoglutarate by D-amino acid aminotransferase (D-aAT,[1] EC 2.6.1.21) or racemization by glutamate racemase (EC 5.1.1.3), alanine racemase catalyzes the reversible isomerization between the isomers of alanine (*5*, *6*, *39*). The presence of D-amino acids in the oligopeptide cell wall linker is purported to serve a role in hindering protease activity.

The mechanism by which alanine racemase facilitates racemization relies on the presence of a diametrically opposed acid/base pair provided by Lys39 (originally bonded to the pyridoxal cofactor via a Schiff base) and Tyr265′[2] from the opposing monomer (*7*−*9*). Upon formation of an initial substrate−PLP aldimine, Lys39 abstracts a proton from the C_α proton in the D-isomer case, while Tyr265′ protonates from the opposite face in a stepwise fashion to generate the L-enantiomer (*8*, *10*−*12*). The opposite is true in the event of L-substrates. An intricate hydrogen bonding network at the active site of alanine racemase [including a carbamylated lysine residue (*13*)] perturbs the pK_a of Tyr265 (∼7.2) such that functionality at physiological pH is feasible (*7*, *10*, *13*, *14*). How the ionization state of the system is regenerated for another round of racemization, however, is unknown.

As a result of the restriction to the bacterial and fungal taxon, alanine racemase provides a target for antibiotics. The D-isomer of cycloserine (4-amino-3-isoxazolidinone) is a natural fungal product and has been reported as an alanine racemase inhibitor for some time (*4*). However, its mechanism of inactivation has only recently been elucidated (*15*−*17*). In the case of both aminotransferases and alanine racemase, cycloserine undergoes an initial transimination/transaldimination to form an external aldimine, leading to a 1,3 prototropic shift in forming a ketimine species (the first step inherent in PLP−transaminase chemistry). This is followed by a second prototropic shift in the formation of a stable isoxazole (*15*−*19*). As the inactivation mechanism requires transaminase chemistry, cycloserine inactivation of alanine racemase provides a useful case study for under-

† This work was supported by a grant from the Molecular and Cellular Biosciences Division of the National Science Foundation.

‡ Coordinates and structure factors have been deposited in the RCSB Protein Data Bank as entries 1XKQ for the D-cycloserine (DCS) and 1XQL for the L-cycloserine (LCS) structures.

* To whom correspondence should be addressed. E-mail: ringe@brandeis.edu.

§ Rosenstiel Basic Medical Sciences Research Center.

|| Program in Biochemistry. Current address: Stanford University, Stanford, CA 94305.

⊥ Program in Biophysics. Current address: Abbott Laboratories, Abbott Park, IL.

⊗ Current address: The University of Kansas Medical Center, Kansas City, KS 66160.

[1] Abbreviations: D-aAT, D-amino acid aminotransferase; CHES, 2-(*N*-cyclohexylamino)ethanesulfonic acid; DAAO, D-amino acid oxidase; DTT, dithiothreitol; LDH, L-lactate dehydrogenase; NAD^+, β-nicotinamide adenine dinucleotide (oxidized); NADH, β-nicotinamide adenine dinucleotide (reduced); PEG, polyethylene glycol; PLP, pyridoxal 5′-phosphate; PMP, pyridoxamine 5′-phosphate.

[2] Residues marked with a prime are donated by the opposing monomer in the dimer.

10.1021/bi047842l CCC: $30.25 © 2005 American Chemical Society
Published on Web 03/15/2005

standing mechanism and stereochemistry, and joins a line of pyridoxal-dependent enzymes which carry out transamination as a side reaction (*20*). It is of pathological interest to note whether the cycloserine reaction scheme may also hold true for serine racemase, a mammalian enzyme found in brain tissue (*3*, *21*).

The first prototropic shift in cycloserine inactivation requires both proper substrate chirality at the C_α position (from which the proton is transferred to cofactor C4′) and an appropriately positioned base to carry out the conversion. As alanine racemase is a two-base (Lys39 and Tyr265′) system, this prototropic shift is observed upon introduction of either cycloserine isomer (*16*). On the other hand, crystallographic studies using a single-base system (dialkylglycine decarboxylase, EC 4.1.1.64) have shown that only L-cycloserine yielded the sp^2 geometry about the C_α position expected of a ketimine, as the D-isomer does not provide the proper chirality for proton abstraction by the active site lysine (*19*). Here we report kinetic and crystallographic tests using a Y265F mutant of *Bacillus stearothermophilus* alanine racemase to test the inactivation efficacy of both cycloserine isomers upon removal of one of the required catalytic bases. While Tyr265 may not be directly responsible for carrying out inactivation per se, it has been suggested to serve a critical role in controlling alanine racemase chemistry to favor racemization over such side reactions as the prototropic shift inherent in cycloserine inactivation (*1*, *16*, *22*). Tyr265 is further believed to play a role in the transaldimination reaction required to form the initial external Schiff base with substrate (*10*).

Independent results indicate this mutant is 1600-fold slower at catalyzing racemization than the wild type, supporting the necessity of Tyr265 for a two-base mechanism (*1*). However, the results presented here show that D-cycloserine in the presence of Y265F alanine racemase loses the 420 nm maximum (corresponding to the aldimine species) 3−10 times faster than the wild-type enzyme in a second-order rate process and inactivates 10 times slower than the wild type, suggesting the importance of Tyr265 in controlling kinetics at both the transaldimination and final inactivation step, albeit in an opposing manner. On the other hand, L-cycloserine-derived kinetics demonstrate a biphasic loss of 420 nm absorbance and activity, suggesting two different binding modes. One mode may be similar to D-cycloserine binding (a binding mode possible due to the loss of the bulky hydroxyl group on Tyr265), leading to a rapid 420 nm absorbance loss (compared with wild-type results) and inactivation. The second binding mode we observe most likely requires Tyr265 to act in aldimine formation and racemization, a process blocked by the mutation. Therefore, the second binding mode leads to slow formation of the geminal diamine and several possible inactivation pathways that arise as a result of the loss of Tyr265. From these data, we propose Tyr265 is involved in several crucial steps along the substrate binding, racemization, and isoxazole formation pathway. More importantly, the degree to which each step requires Tyr265 depends on the initial chirality of the substrate or inhibitor, which yields complicated kinetic pathways. This provides for a difficult task with regard to antibiotic drug design. Nevertheless, these data allow for the further characterization of the cycloserine inactivation pathway in the case of alanine racemase.

EXPERIMENTAL PROCEDURES

Materials. D/L-Cycloserine, D-alanine, L-alanine dehydrogenase, and NAD^+ were purchased from Sigma (St. Louis, MO). D-Alanine was purchased from Aldrich (Milwaukee, WI). CHES buffer and PEG 4K were purchased from Fluka (St. Louis, MO).

Mutant Preparation. Alanine racemase mutagenesis was carried out using the QuickChange site-directed mutagenesis kit (Stratagene, La Jolla, CA). Plasmid DNA was isolated from *Escherichia coli* strain DE3 transformed with pET21a containing the *B. stearothermophilus* alanine racemase construct pMDalr3 using the QIAprep Miniprep Kit (QIAGEN, Valencia Technologies, Carlsbad, CA) (*23*).

Protein Purification. B. stearothermophilus alanine racemase was prepared as described previously (*13*). The purified enzyme was run over a Bio-Gel P-6DG (Bio-Rad) column (2 cm × 45 cm) equilibrated and eluted with 100 mM Tris-HCl buffer (pH 8.5) containing 1 mM DTT and 10 μM PLP. Protein was concentrated using Amicon concentrators with a 10 kDa molecular mass cutoff.

Crystallization. Alanine racemase crystals (0.6 mm × 0.6 mm × 0.5 mm) were grown by the hanging drop method. The hanging drop contained 5 μL of the protein solution (concentrated to 25 mg/mL), 5 μL of 23% (w/v) PEG 4K, 200 mM sodium acetate, a range of 0−4.5% acetone and/or 0−1% benzamidine, and 100 mM Tris (pH 8.5). Drops were equilibrated against 700 μL of the PEG 4K solution. Crystals grown in this fashion have a distinct yellow color due to the presence of PLP in an aldimine linkage (*11*, *13*). Stock solutions of 100 mM D- and L-cycloserine were prepared using the components from the well solution, and exchanged into drops containing crystals in 2 μL steps over the course of 1 h.

Data Collection and Processing. B. stearothermophilus alanine racemase crystallizes in space group $P2_12_12_1$, and contains a dimer in the asymmetric unit. All diffraction data were collected using an in-house Cu Kα rotating anode source (RU-300B) running at 40 kW and 30 mA equipped with a RAXIS-IV image plate detector. Data for enzyme crystals treated with D-cycloserine were collected under cryo conditions (using 30% glycerol as a cryoprotectant), while data for enzyme crystals treated with L-cycloserine were collected at room temperature. Diffraction data were integrated, scaled, and merged using the HKL software package (*24*). Processing statistics for the two data sets are outlined in Table 1.

Structure Solution and Refinement. For both data sets, the native structure as a dimer was used as the starting model (PDB entry 1SFT), excluding waters, bound PLP, acetate, and Tyr265 (modeled initially as an alanine to preserve connectivity) (*11*). Refinement was carried out to 1.95 and 1.8 Å in the case of D- and L-cyloserine, respectively. A subset of the data was set aside for cross validation (5%), and all refinement was carried out using a maximum likelihood amplitude-based target function as implemented in the CNS package (*25*, *26*). Refinement statistics for both data sets are summarized in Table 1.

The initial refinement consisted of rigid body refinement (treating each monomer independently) followed by simulated annealing torsion-based dynamics. Repeated rounds of conjugate energy minimization and restrained, individual

Table 1: Y265F Alanine Racemase Data Processing and Refinement Statistics

	DCS	LCS
space group	$P2_12_12_1$	$P2_12_12_1$
unit cell		
a (Å)	84.97	98.8
b (Å)	85.63	89.8
c (Å)	97.96	85.2
resolution range (Å)	50.0−1.8	50.0−1.95
no. of reflections (unique)	608518 (66943)	681383 (91451)
I/σ (highest-resolution shell)	8.9 (2.1)	9.8 (3.2)
completeness (highest-resolution shell)	88.8 (84.2)	90.9 (97.6)
R_{merge}[a] (%) (highest-resolution shell)	9.4 (46.7)	9.5 (30.0)
R_{factor} (R_{free})[b] (%)	19.1 (24.0)	17.8 (20.7)
no. of protein residues	760 (380 per monomer)	760 (380 per monomer)
no. of water atoms	476	331
average *B* factor	27.9	27.3

[a] $R_{merge} = \sum|I_{obs} - I_{avg}|/\sum I_{obs}$. [b] $R_{factor} = \sum||F_{obs}| - |F_{calc}||/\sum|F_{obs}|$. See Brunger (*25*) for a description of R_{free}.

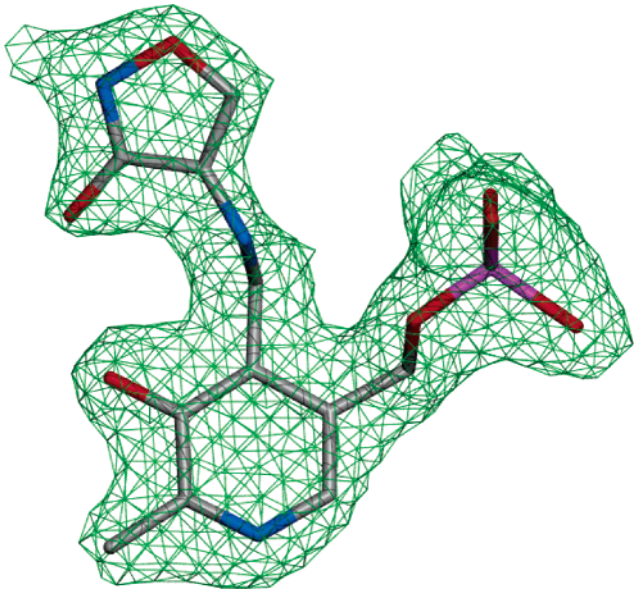

FIGURE 1: D-Cycloserine-soaked Y265F alanine racemase σ_A-weighted electron density maps with $F_o - F_c$ coefficients (contour, 2.0σ) at the active site. All atoms shown are from the final refined model, and were not included prior to the phase calculation for the shown maps. All figures were generated using POVScript+ (*38*) and rendered using POVRay (http://www.povray.org).

temperature factor minimization were interspersed with manual inspection of σ_A-weighted electron density maps using O (*27, 28*). Before possible adducts at the active site were evaluated, water picking and side chain modifications or corrections were manually performed to improve model phases. In the case of D-cycloserine, $F_o - F_c$ difference maps were consistent with a closed, planar cycloserine ring (Figure 1), and appropriate parameters for this adduct were used in further refinement rounds. Electron density maps in the L-cycloserine case suggested the presence of PMP, acetate, and bound L-cycloserine in addition to the closed ring species (Figure 2). PMP/acetate, L-cycloserine, and the closed ring species were refined as alternate conformers with split occupancies to avoid steric clashes.

Pyruvate Rescue. Following incubation of Y265F alanine racemase (300 μM) with either enantiomer of cycloserine (10 mM for D and 40 mM for L) as described in UV−Vis Spectroscopy, enzyme solutions were allowed to sit for 1 h, after which a second time-dependent absorbance recording at 420 nm was collected to ensure the completion of modification. These solutions were then passed over a P-6DG column to remove excess inhibitor. Pyruvate was added to each solution (150 mM), and absorbance recordings were taken at time points immediately following, 24, 48, and 72 h post addition (Figure 3). Controls in which no pyruvate was added were also performed.

Enzyme Assays. Enzyme activity was followed at 37 °C in the D → L direction using a coupled assay system with L-alanine dehydrogenase (*29*). Assays were performed in 0.5 mL cuvettes containing 100 mM CHES buffer (pH 9.1), including 5 mM NAD^+, 3 units of L-alanine dehydrogenase (1 unit converts 1 μmol of L-alanine to pyruvate and NH_3 per minute at pH 10 and 25 °C), and 400 mM D-alanine. Reactions were initiated by adding the desired amount of alanine racemase and monitoring the appearance of NADH at 340 nm (using an ϵ of 6220 M^{-1} cm^{-1}).

Inactivation Kinetics. Inactivation of Y265F alanine racemase was assessed by incubating the mutant enzyme (10 μM) with the desired concentration of D- or L-cycloserine (in all cases, [I] ≫ [E] for observation of pseudo-first-order behavior). At periodic intervals, 20 μL aliquots of the inactivation mixture were quenched in 475 μL of the assay solution (as described in Enzyme Assays). The rate of activity was plotted as a function of cycloserine concentration and fit to a hyperbolic response using a Michaelis−Menten type equation [k_{obs}[I]/(K_i + [I]) (Figure 4)].

UV−Vis Spectroscopy. In all spectroscopy experiments, t_0 refers to the time at which cycloserine is introduced in solution. Broad wavelength (300−500 nm) scans of Y265F alanine racemase were recorded at 1 min intervals for 20 min using the purified enzyme (10 μM) following addition of either 50 μM D-cycloserine or 1 mM L-cycloserine. Experiments were referenced against a solution lacking cycloserine. In a separate set of experiments, varying concentrations of cycloserine were added to the mutant enzyme (10 μM), and the change in absorbance at 420 nm was monitored at 1 s intervals for 10−20 min. Changes in absorbance (relative to absorbance at t_0 and using the absorbance at t_∞ as a baseline) were plotted as a function of time and fit to second- or third-order decay processes (i.e., two or three exponentials, Figure 7 or 8, respectively) in the case of D- and L-cycloserine, respectively.

RESULTS AND DISCUSSION

Experiments performed thus far regarding L-cycloserine inactivation of alanine racemase suggest the necessity of two catalytic bases (Lys39 and Tyr265′) for the achievement of the isoxazole end product (*16*). Because of this stereochemical requirement, detectable differences are observed in inactivation rates of the two isomers. Further, studies performed using single-base PLP-dependent systems (e.g., decarboxylases and transaminases) imply that the stereochemistry about the α-carbon of cycloserine is crucial to achieving the initial prototropic shift, as the C_α proton must be in the proper orientation to permit access by the catalytic base (*19*). This begs the question of how Tyr265 mutants would affect inactivation kinetics and mechanisms, and what this information yields with regard to inhibitor design.

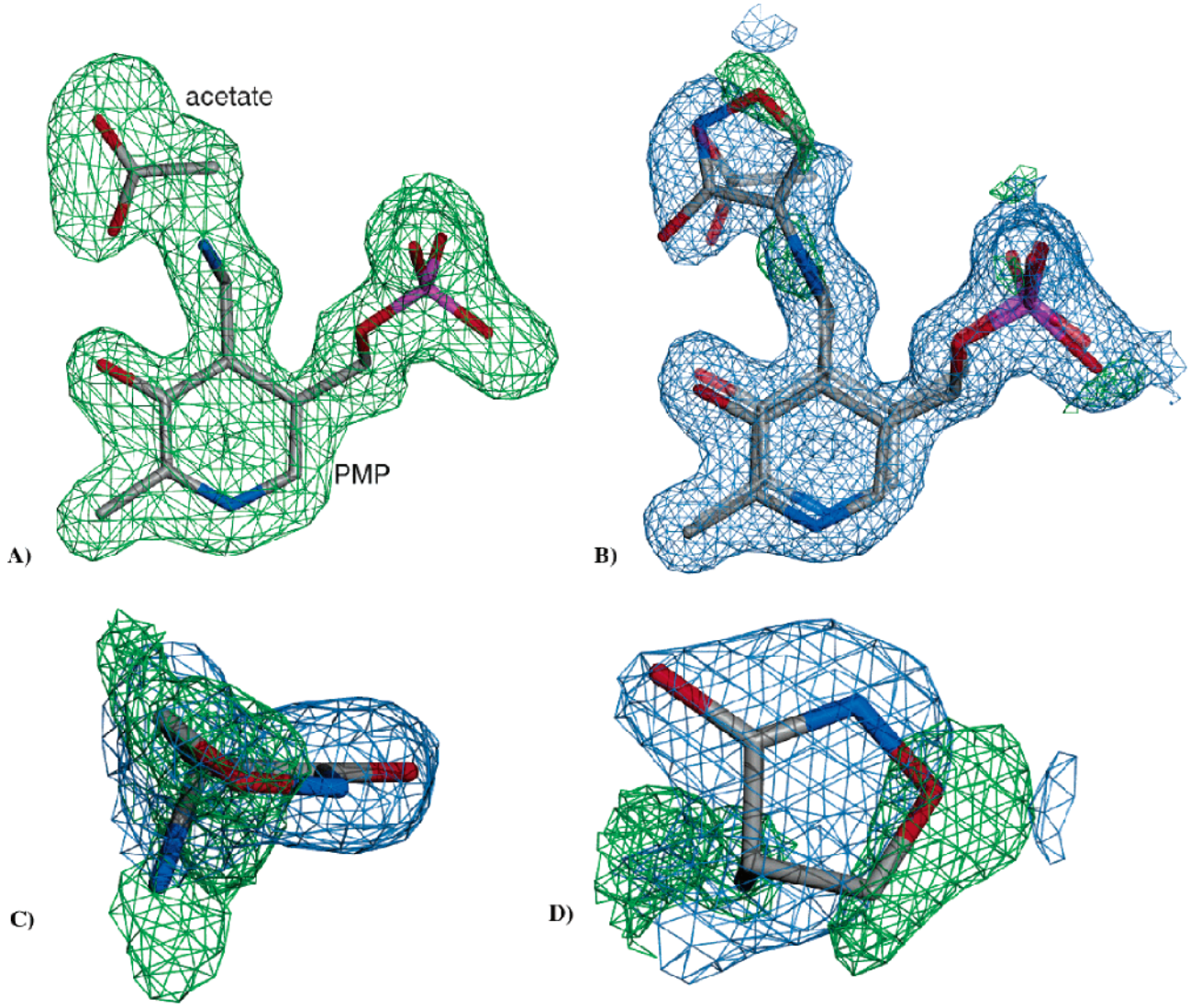

FIGURE 2: L-Cycloserine-soaked Y265F alanine racemase σ_A-weighted electron density maps with $F_o - F_c$ coefficients (green; contour, 2.0σ) and $2F_o - F_c$ coefficients (blue; contour, 1.0σ). (A) Maps shown before inclusion of the PMP and acetate model in the refined phases. After refinement of PMP and acetate in the model, residual density is apparent near the acetate molecule that is consistent with either the closed ring species (B) or L-cycloserine bound in the Michaelis complex (C and D).

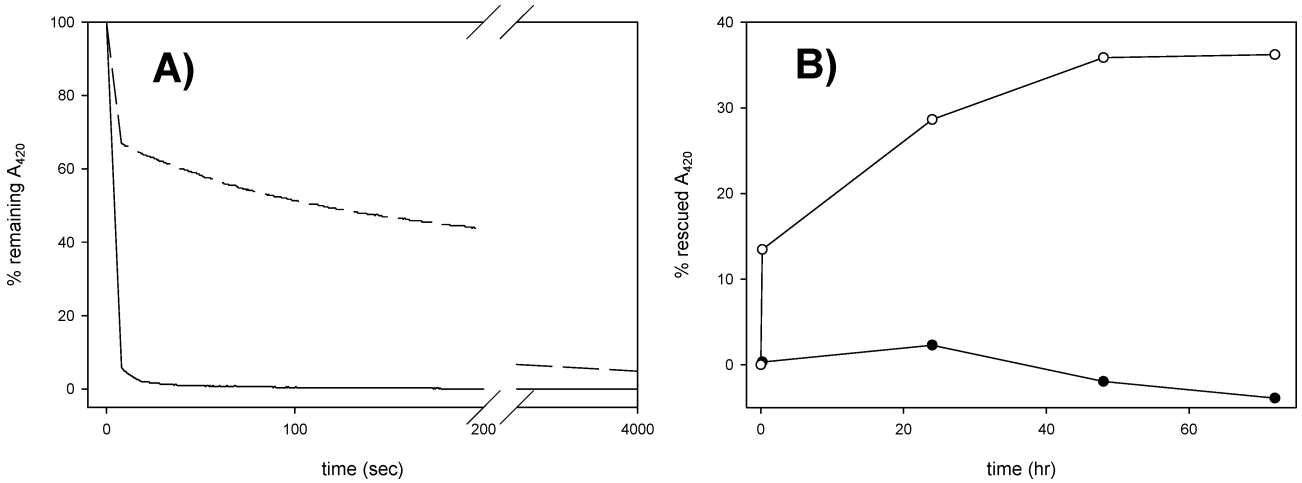

FIGURE 3: PMP rescue experiments. (A) Addition of D-cycloserine (10 mM, solid curve) or L-cycloserine (40 mM, dashed curve) before addition of pyruvate. (B) Addition of pyruvate (150 mM) to either D-cycloserine (●) or L-cycloserine (○) after removal of cycloserine via gel filtration.

Cycloserine−Mutant Enzyme Complexes. Crystallographic structures of both D- and L-cycloserine-inactivated Y265F alanine racemase complexes were determined to 1.95 and 1.8 Å, respectively. In the former case, electron density maps with $F_o - F_c$ coefficients clearly indicate the presence of a planar isoxazole ring, similar to that seen in the wild-type

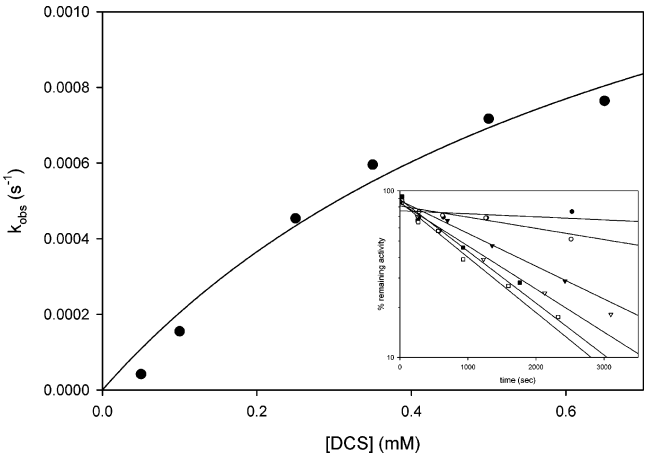

FIGURE 4: Hyperbolic fit to activity loss as a function of D-cycloserine concentration (range of 0.05−0.65 mM). The inset shows the raw data overlaid with linear fits.

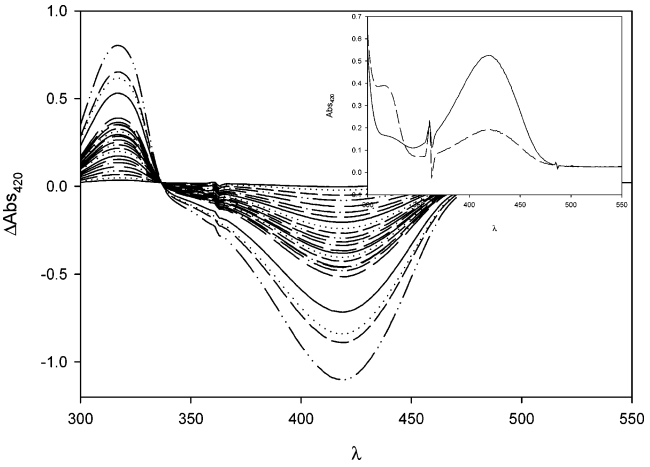

FIGURE 5: Photodiode scans of Y265F alanine racemase upon addition of 50 μM D-cycloserine. The baseline was set to zero before addition of cycloserine. The inset shows t_0 (solid line) and t_f (dashed line) scans using buffer as the baseline.

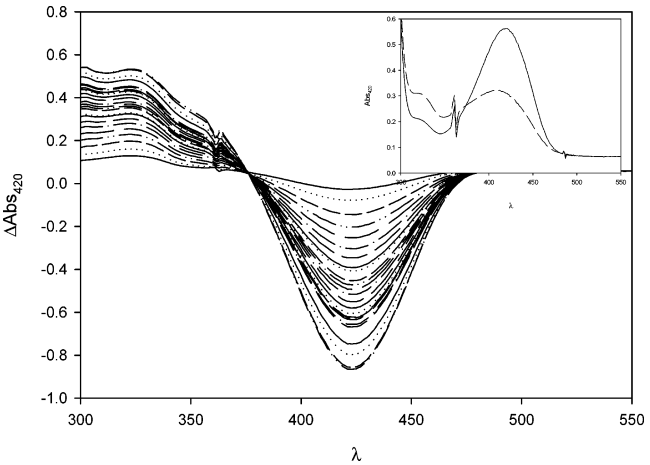

FIGURE 6: Photodiode scans of Y265F alanine racemase upon addition of 1 mM L-cycloserine. The baseline was set to zero before addition of cycloserine. The inset shows t_0 (solid line) and t_f (dashed line) scans using buffer as the baseline.

cycloserine-inactivated alanine racemase complex (Figure 1) (*16*). This further implies a like pathway of inactivation in the mutant and wild-type enzymes in the presence of D-cycloserine. The L-cycloserine complex, however, suggested either a ring-opened form of cycloserine, pyridoxamine (PMP), in the presence of acetate or a combination of the two. The presence of acetate is most likely derived from the crystallization buffer, as the carboxylate binding pocket of alanine racemase has been known to bind such molecules (*11*, *13*). Because of the ability to rescue the L-cycloserine-inactivated enzyme with pyruvate (the α-keto acid of alanine, vide infra) and the potential reactivity of an open ring form of cycloserine (discussed in more detail below), PMP and acetate were modeled in this density (Figure 2A). Upon refinement of this model, $F_o - F_c$ maps

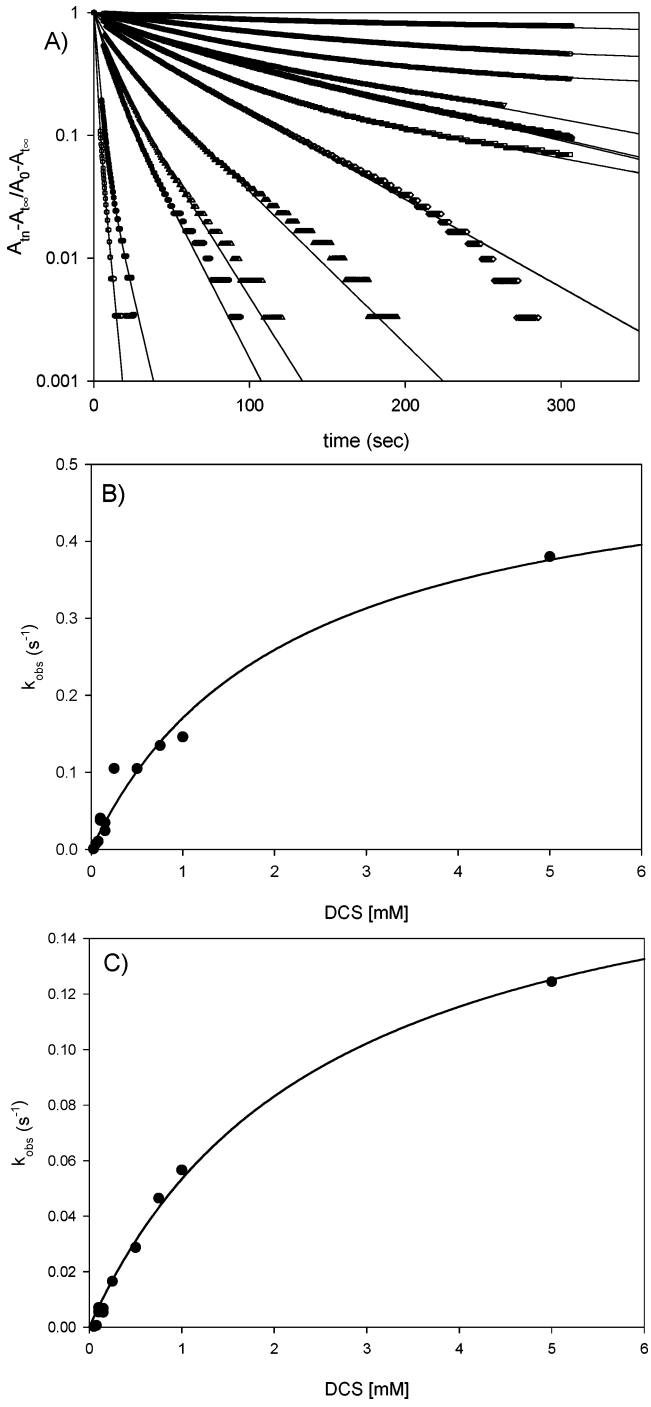

FIGURE 7: Spectral changes and respective fits at 420 nm as a function of D-cycloserine concentration (range of 0.025−5 mM) upon incubation with Y265F alanine racemase. (A) Raw data overlaid with double-exponential fits. Exponential factors (constrained to sum to 1.0) are plotted in panels B and C and fitted with hyperbolic saturation curves.

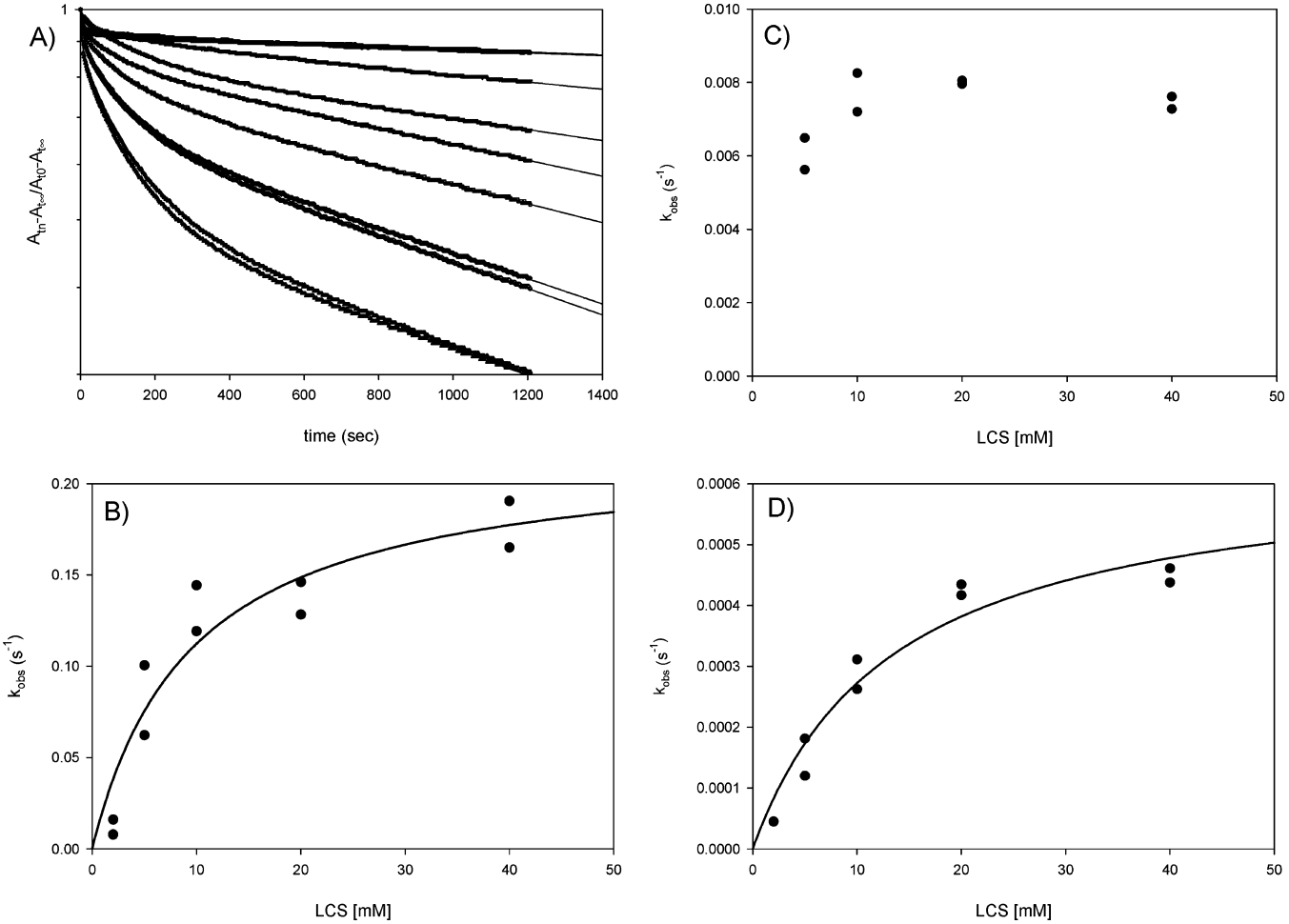

FIGURE 8: Spectral changes and respective fits at 420 nm as a function of L-cycloserine concentration (range of 2−40 mM) upon incubation with Y265F alanine racemase. (A) Raw data overlaid with triple-exponential fits. Exponential factors (constrained to sum to 1.0) are plotted in panels B−D. Only panels B and D were fitted to hyperbolic saturation curves.

indicated residual density near the acetate species consistent with a closed ring adduct (Figure 2B) or L-cycloserine bound in the Michaelis complex (Figure 2C,D). As the Y265F variant retains 0.1% of the activity of the wild type (*1*, *30*), the presence of some cycloserine-derived isoxazole is not surprising. However, the presence of L-cycloserine in the Michaelis complex suggests one of two possibilities: either the base responsible for formation of the geminal diamine is hindered in some fashion, or this structure represents an alternative mode of binding such that accessibility from the base to the amine group of cycloserine is not permitted. Therefore, PMP, L-cycloserine, and the isoxazole were included in the model, although PMP is most likely the dominant species (i.e., of higher occupancy; however, occupancies of the two were not refined given the resolution of the data). In both the D- and L-cycloserine-inactivated complexes, the overall topology of the active site is similar to that of the native enzyme, thereby indicating the inhibitor did not significantly perturb the geometry about the active site.

The final models were subjected to PROCHECK analysis to assess model quality (*31*). The D-cycloserine model has 602 residues (90.8%) in the most favored regions, 57 residues (8.6%) in additionally allowed regions, and four residues (0.6%) in generously allowed regions. Analysis of these four residues (Phe215 and Ser264 from each monomer) indicated unambiguous placement of the atoms in σ_A-weighted electron density maps with $2F_o - F_c$ coefficients, so no alterations were made to their atomic positions. Further, these outliers are consistent with previous results (*8*, *13*). The L-cycloserine model was very similar, with 605 residues (91.3%) in the most favored regions, 54 residues (8.1%) in additionally allowed regions, and the same four residues (0.6%) in generously allowed regions. No residues were in disallowed regions of the Ramachandran plot for either structure.

Pyruvate Rescue. The crystallographic data derived from Y265F complexed with L-cycloserine indicate either the presence of an opened cycloserine ring (such as that shown by mechanism 7 in Scheme 1) or some form of PMP together with acetate from the crystallization buffer (Figure 2). In the case of the latter, this can be tested via addition of the α-keto acid of alanine, which would undergo a transamination reaction [albeit potentially rarely given the preference for racemization (*22*)] to regenerate the Schiff base. This would lead to an increase in the 420 nm absorbance corresponding to the rescue of the aldimine, supporting the results suggesting the formation of PMP. In contrast, Y265F alanine racemase incubated with D-cycloserine should not show this effect, as the structural results do not support the presence of PMP at the active site (Figure 1). Figure 3A illustrates the effect of adding cycloserine, resulting in the loss of the 420 nm absorbance until an equilibrium is reached with each isomer (roughly 5% of the original A_{420}). After removal of cycloserine via gel filtration, pyruvate was added

Scheme 1: Proposed Cycloserine Inactivation Mechanism with Y265F Alanine Racemase[a]

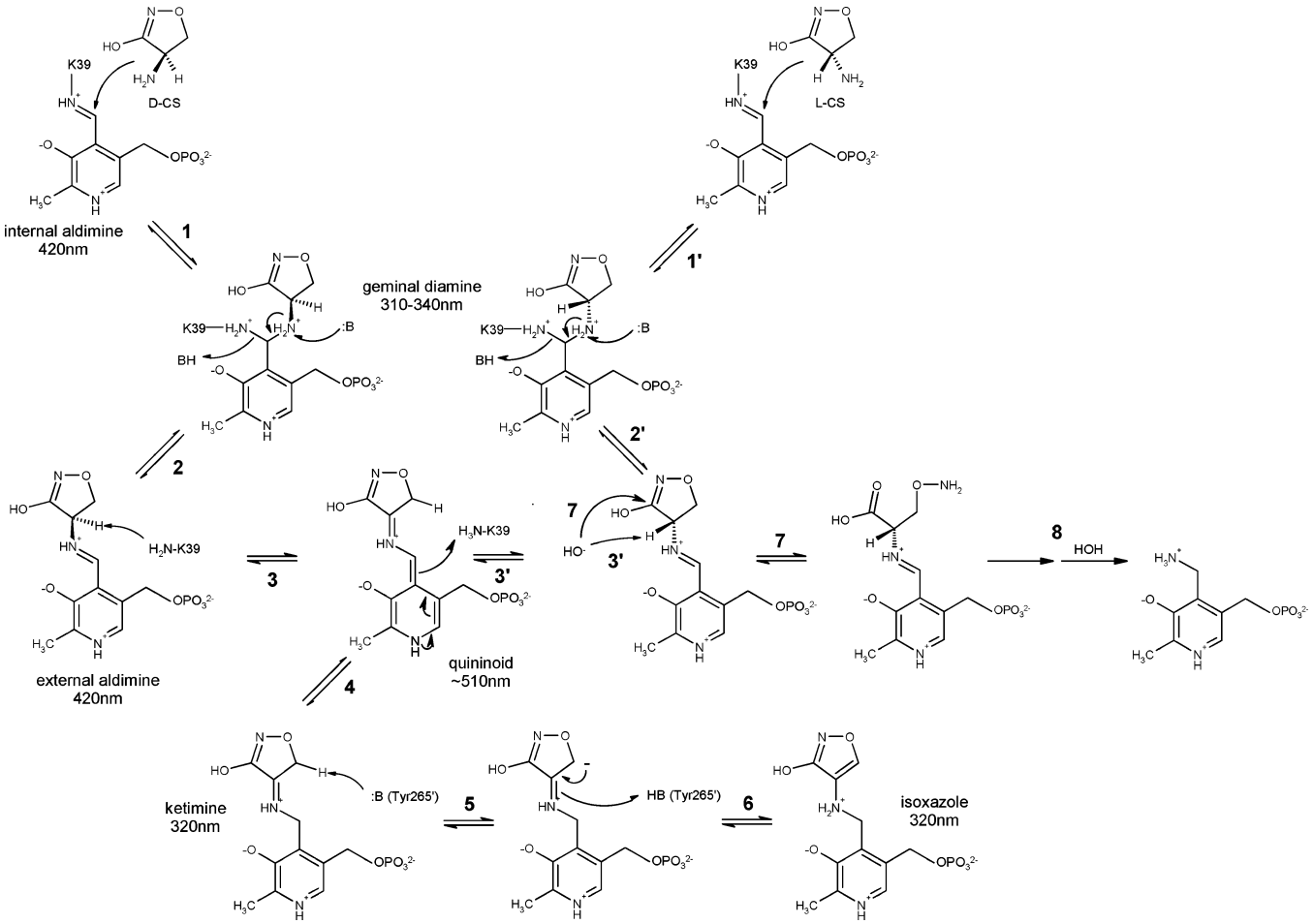

[a] Only the inactivation process is shown from the quininoid species for the sake of clarity.

(Figure 3B) to each solution. In the case of D-cycloserine, no apparent effect on the absorbance at 420 nm was observed, even after 72 h [Figure 3B (●)]. Conversely, pyruvate had an immediately measurable effect following L-cycloserine derivitization [Figure 3B (○)], which continued over the course of 48 h before reaching an equilibrium roughly corresponding to the amount of enzyme not affected by the burst phase (approximately 35%), which seems to agree with the crystallographic results indicating some enzyme forming the inactivated isoxazole species (Figure 2). Additional control experiments in which pyruvate addition was omitted following cycloserine removal did not show an increase in A_{420} (data not shown). The formation of the PMP adduct suggested by the crystallographic results is supported by the UV−vis data, as only the L-cycloserine-inactivated enzyme shows a broadening in the peak at ~320 nm (most likely derived from a mixture of both the closed ring form and PMP, vide infra) (*32*).

Kinetics of Inactivation. A straightforward means of analyzing the form of PLP bound to the enzyme is spectroscopic analysis, as the different ionic forms of the coenzyme have significantly different spectral properties (*32*). Therefore, as the crystallographic experiments suggest the presence of two to three species in the case of inactivation with L-cycloserine, spectroscopic analysis of the mutant enzyme in the presence of inhibitor may also support this notion. Inactivation kinetics using D-cycloserine performed under pseudo-first-order conditions were plotted as a function of concentration and fit to an apparent first-order rate constant, yielding an inactivation rate of 1.4×10^{-3} s^{-1} (Figure 4 and Table 2). Similar experiments were performed with L-cycloserine, although the complexity of the process allowed an only qualitative assessment of inactivation. The inactivation process appeared to be biphasic, with a rapid burst phase followed by a slower phase that was difficult to adequately measure given the technical limitations of the assay system. After incubation with L-cycloserine for approximately 45 min, Y265F alanine racemase retained 98, 83, 63, 57, and 49% activity using 1.0, 2.0, 5.0, 10.0, and 20.0 mM inhibitor, respectively (data not shown). The appearance of a second-order (or higher) inactivation process agrees with the crystallographic results, as the presence of different species at the active site implies multiple pathways.

Table 2: Alanine Racemase Kinetics for the Wild Type and Y265F[a]

	DCS		LCS	
	k_{obs} ($\times 10^{-3}$)	K_i	k_{obs} ($\times 10^{-3}$)	K_i
wt[b] Δ_{420}	≫43	≫10	6.0 ± 0.4	8.6 ± 1.3
wt[b] enzyme inactivation	>9	>4	1.0 ± 0.1	6.0 ± 1.8
Y265F Δ_{420} (k_1)	540 ± 50	2.1 ± 0.4	220 ± 30	9.6 ± 3.5
k_2	190 ± 10	2.5 ± 0.3	0.6 ± 0.1	14 ± 4
Y265F enzyme inactivation	1.4 ± 0.07	0.33 ± 0.08	−	−

[a] All rates are in units of s^{-1}, and equilibrium constants are in units of mM. [b] wt data are corrected values from Fenn et al. (*16*).

To further explore the Y265F inactivation pathway in the context of cycloserine, spectroscopic profiles of the cofactor during the course of the reaction were monitored. Initial spectra exhibit the characteristic peak at 420 nm due to a Schiff base linkage between Lys39 and the cofactor (insets of Figures 5 and 6, t_0 scan). Upon addition of D-cycloserine, Y265F alanine racemase exhibits a behavior similar to that seen in the wild-type case, a rapid decrease in the aldimine absorbance (420 nm) with a concomitant increase at 320 nm (isosbestic point, 337 nm) (Figure 5), consistent with a saturated C4′ position on the cofactor (*32*). Comparatively, L-cycloserine yields a broadened spectrum in the 320 nm regime and an isosbestic shift 56 nm upfield (Figure 6). This is consistent with the formation of different end products in the case of D- versus L-cycloserine, as suggested by the crystallographic and inactivation experiments.

It is also of interest to note that the described spectral changes required vastly different concentrations of cycloserine, 50 μM and 1 mM in the D- and L-cycloserine experiments, respectively. When the absorbance loss at 420 nm was monitored as a function of time, D-cycloserine experiments show a rapid loss by addition of <1 mM inhibitor (Figure 5, inset). Fits of these data to hyperbolic saturation curves yield two rates (i.e., two exponentials) of absorbance loss of 190×10^{-3} and 540×10^{-3} s^{-1} (Figure 7 and Table 2). On the other hand, experiments utilizing L-cycloserine required concentrations of up to 40 mM prior to full saturation (Figure 6, inset). These data required three exponentials to be adequately fit (except for the lowest cycloserine concentration, where the convergence of only two of the exponentials was successful), two of which can be fit to a hyperbolic response (Figure 8 and Table 2).

Y265F Cycloserine Inactivation Mechanism. Recent evidence suggests racemization proceeds via a stepwise process, which is assumedly also true for cycloserine and requires a modification of the current cycloserine inactivation scheme (*10*, *16*). Given a stepwise racemization, differences in absorbance at 420 nm must arise at a step prior to quininoid formation, as all steps following this intermediate are identical. As a buildup in the quininoid spectral maxima (~510 nm) is not observed, the difference in 420 nm absorbance rates must therefore be due to loss of the geminal diamine species formed during transaldimination. This agrees with kinetic and solvent isotope effects using alanine as a substrate, indicating that transaldimination in the L → D direction is slower and primarily rate-limiting as opposed to transaldimination in the D → L direction (*33*). Despite this, geminal diamine species have proven to be difficult to isolate or observe in PLP systems (*34*, *35*). More recent models have instead suggested that conformational fluctuations play a role in rate determination, although this appears to be the case only at pH values near neutrality (*36*).

In light of a rate-limiting transaldimination process, the multiphase rates and the origin of the rate difference must also be rationalized. The crystallographic results provide some clues about possible sources of multiphase rates, as the L-cycloserine data imply the presence of some inhibitor bound to the enzyme but not covalently linked to the pyridoxal cofactor (Figure 2). If these data are analyzed from the standpoint presented in Figure 9, then either Lys39 or Tyr43 appears to be appropriately positioned to act as the base involved in L-cycloserine transaldimination via the

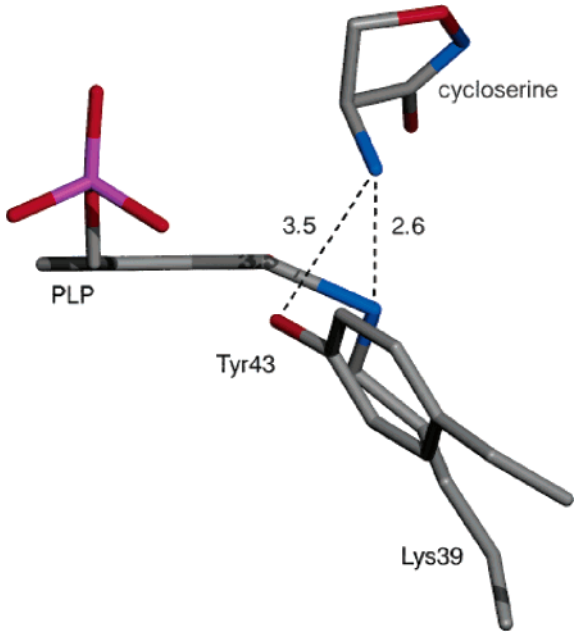

FIGURE 9: Hydrogen bonding network from the amine group of L-cycloserine in the Michaelis complex to Y265F alanine racemase based on the model derived from Figure 2C,D. Only Lys39 and Tyr43 are appropriately positioned to act as catalysts for the formation of the initial geminal diamine (see the text for a discussion). PLP bound in the internal Schiff base configuration via Lys39 is shown for clarity.

geminal diamine intermediate. Previous theories regarding the residue(s) involved in this step were based on only Tyr265′ (*10*). However, it is apparent from comparing Y265F alanine racemase bound to L-cycloserine with wild-type alanine racemase that either His166 or Tyr265′ may act in this role, and only in the case where stereochemistry of the α-carbon is inverted, i.e., that of the D-isomer (Figure 10). This therefore suggests the possibility of two different binding modes for cycloserine (at least in the case of Y265F alanine racemase), thereby providing a means by which two differing rates may arise.

If the model shown in Figure 10 is correct, then the amine group of cycloserine would be in close contact with Tyr265′ such that steric hindrance may alter the rate of geminal diamine formation. This model may explain the *increase* in rate of spectral loss at 420 nm in the case of the mutant versus wild-type enzyme in the case of D-cycloserine. In the wild-type case, Tyr265′ may be required for only racemization, while His166 may be the major player in formation of the geminal diamine species (and potentially transaldimination in general), although steric hindrance between the substrate and Tyr265′ may weaken interactions between His166 and the substrate. Additionally, Tyr265 may perturb the pK_a of the surrounding groups such that transaldimination is disfavored. Either of these cases would yield the observed increase in the rate of geminal diamine formation observed here in the event of D-cycloserine bound to the Y265F mutant. It is difficult to assign the biphasic nature of the 420 nm loss to mechanistic roles in the D-cycloserine case; one rate may represent formation of the geminal diamine, while the second represents an alternative binding mode or loss of the external aldimine species (both at rates faster than that of the wild-type enzyme).

In contrast to the increase in the rate of spectral loss at 420 nm in the Y265F versus wild-type enzyme, the rate of

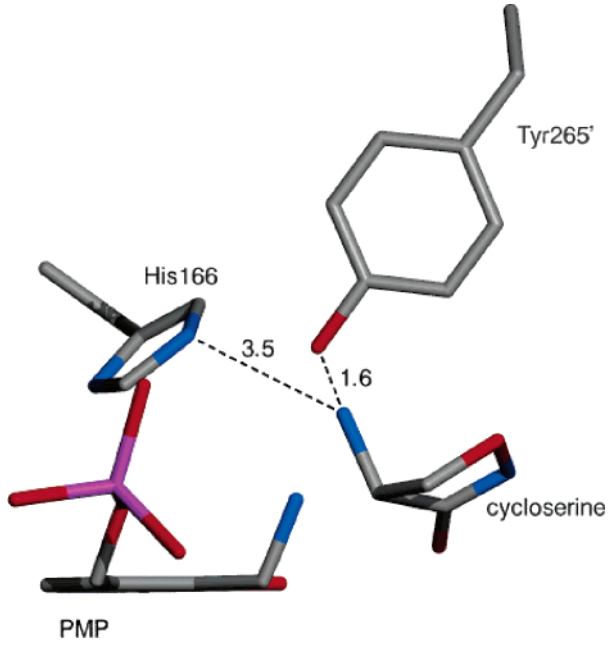

FIGURE 10: Model of the D-cycloserine hydrogen bonding network from the amine group of D-cycloserine in the Michaelis complex to wild-type alanine racemase. The model was generated by superpositioning Y265F alanine racemase bound to L-cycloserine with wild-type alanine racemase, followed by inversion of the stereochemistry about the α-carbon of cycloserine. In this instance, His166 and Tyr265′ are appropriately positioned to aid in formation of the geminal diamine species. PMP from the Y265F structure bound to L-cycloserine is shown for clarity.

Y265F enzyme inactivation *decreases* approximately 10-fold versus that of the wild type (Table 2). This suggests Tyr265 is responsible for some step following formation of the ketimine, which seems reasonable given the distances to the cofactor in the wild-type studies (*16*). Interestingly, this implies Tyr265 plays a dual role as a regulator of racemization (vide infra) and inactivation itself. This complicates matters with regard to drug design, as candidates that attempt to exploit Tyr265 may have several effects on the mechanism of action.

The spectral studies utilizing the mutant enzyme and L-cycloserine are more complicated, as both the spectral and inactivation rates suggest a multiphase process. It is interesting to note that the burst phase in the Y265F with L-cycloserine Δ_{420} experiment (k_1) is similar in magnitude to rate k_2 in the analogous Y265F with D-cycloserine experiment (220 and 190 s^{-1}, respectively; Table 2). This suggests this rate may be reflective of a similar process, such as an alternative binding mode for L-cycloserine that allows His166 to facilitate transaldimination (similar to that illustrated in Figure 10). Alternative binding modes seem reasonable given the lack of the bulky hydroxyl group from Tyr265. Such a form of binding may also explain the apparent biphasic loss of racemase activity, as the binding mode shown in Figure 10 would position Lys39 for inactivation without the need for Tyr265′, thereby giving rise to a second mechanism of inactivation. The crystallographic data also support this result, as some evidence for the planar isoxazole is evident in the electron density maps (Figure 2). Therefore, one of the slower rates of 420 nm loss (rate k_2 in Table 2) most likely arises from the "native" form of binding shown in Figure 9. In this case, Lys39 and Tyr43 are poor at carrying out the initial substrate binding event (i.e., formation of the geminal diamine) compared with His166 and Tyr265′, which could account for a rate-limiting step in the case of L-substrates. Upon formation of the external aldimine, the lack of a sufficient base (i.e., Tyr265′) in this form of binding leads to an extremely slow deprotonation step for the purposes of inactivation or racemization (thereby causing the indeterminable inactivation rate for L-cycloserine), thereby opening the possibility for alternative processes such as ring opening and PMP formation to occur (*1*, *30*). However, it is difficult to assign the remaining rates of 420 nm loss (k_2 or the apparently nonhyperbolic response, Table 2 and Figure 8) to either of these possibilities. It is also possible that the burst phase described reflects the presence of some contaminating D-cycloserine. Given the purity of the synthetic L-enantiomer (99% as given by the vendor) and its slow rate of conversion by alanine racemase compared with that of D-cycloserine, this possibility cannot be ruled out.

A modified version of the cycloserine inactivation mechanism including the Y265F data is shown in Scheme 1. Pathways 1/1′ and 2/2′ may consist of multiple binding possibilities (via His166 and Tyr265′ and/or Lys39 and Tyr43), thereby yielding different rates of inactivation and 420 nm loss (this is indicated in Scheme 1 by the use of B to indicate a number of possible bases). Y265F alanine racemase shows a drop of approximately 1600-fold in terms of catalytic activity (*1*, *30*), yet the presence of 0.1% residual activity in these mutants implis the possibility of solvent-derived base racemization in the case of L-cycloserine (pathway 3′), which seems feasible given the pH for kinetic and crystallization experiments is ≥8.5. As this pathway is most likely reduced by several orders of magnitude, this leaves open the possibility of base-directed hydrolysis of the cycloserine ring, potentially followed by decarboxylation or a prototropic shift and subsequent hydrolysis (pathway 7 followed by pathway 8 in Scheme 1). This suggests an important role for Tyr265 as a major regulator of racemization, as it plays a key role in forcing the chemistry down the racemization path before alternative pathways are ever borne out. Pathways 7 and 8 are similar to the previously suggested means of cycloserine inactivation of PLP-dependent enzymes, which include the possibility of enzyme acylation at the lactim portion of the ring, with the modification in this case to *hydrolysis* of the lactim ring (*37*). No known evidence is currently available for any PLP-dependent enzyme indicative of the acylation pathway in the case of cycloserine inactivation.

The rate of D-cycloserine-derived inactivation indicates a decrease in rate by an order of magnitude in the Y265F experiments (Table 2). This suggests Tyr265 is necessary for the final 1,3 prototropic shift required to form the stable isoxazole (pathway 5 or 6 in Scheme 1). This seems reasonable given the >4 Å distance from Lys39 to the C_α position on cycloserine (data not shown).

Y265F alanine racemase shows a preference for D-cycloserine in terms of inactivation, evidenced both structurally and kinetically. Tyr265 mutation studies performed independently using alanine as a substrate suggest a similar result (*22*). Wild-type assays using various suicide substrates are consistent with an increased rate of inactivation for D-substrates (*29*). We attribute this difference to a different mode of binding for formation of the external aldimine in the case of D-substrates (which may utilize His166 and

Tyr265′ vs Lys39 and Tyr43 in the case of L-substrates). However, this is the first case using cycloserine in which different end products are observed dependent upon initial inhibitor chirality, which we attribute to the requirement for Tyr265 in binding, racemization, and the prototropic shift leading to inactivation. Further, it appears the initial transaldimination process may play an integral role in determining the inactivation process and/or rate. Therefore, molecules which specifically utilize Lys39 as the basis of transaldimination *and* inactivation while discouraging protonation by Tyr265 at C_α (exploiting differences in either p*K* values or geometric restrictions) should increase the efficacy of antibiotics by decreasing the potential for racemization. This may partly explain why cycloserine is an effective inhibitor even in the instance of the wild-type enzyme (*16*). It should also be possible to reverse this logic such that Tyr265 is exploited; this has the potential added benefit of specificity for PLP-containing enzymes with a base properly positioned for such substrates (thereby avoiding single-base-utilizing enzymes). This strategy is not without precedent: Thornberry et al. have reported halovinylglycines that seem to operate through such a mechanism (*40*), although the potential uses of such inhibitors *in vivo* has yet to be fully explored.

ACKNOWLEDGMENT

We thank Alon Yarkoni and Anthony Morollo for preparing and providing the Y265F alanine racemase construct. We also thank Michael Toney and Michael Spies for experimental suggestions and technical assistance. Lizbeth Hedstrom provided the diode array spectrometer, as well as several experimental and manuscript suggestions.

REFERENCES

1. Watanabe, A., Yoshimura, T., Mikami, B., and Esaki, N. (1999) Tyrosine 265 of alanine racemase serves as a base abstracting α-hydrogen from L-alanine: The counterpart residue to lysine 39 specific to D-alanine, *J. Biochem. 126*, 781−786.
2. Dunlop, D. S., Neidle, A., McHale, D., Dunlop, D. M., and Lajtha, A. (1986) The Presence of Free D-Aspartic Acid in Rodents and Man, *Biochem. Biophys. Res. Commun. 141*, 27−32.
3. Hashimoto, A., Nishikawa, T., Hayashi, T., Fujii, N., Harada, K., Oka, T., and Takahashi, K. (1992) The presence of free D-serine in rat brain, *FEBS Lett. 296*, 33−36.
4. Strominger, J. L., Izaki, K., Matsuhashi, M., and Tipper, D. J. (1967) Peptidoglycan transpeptidase and D-alanine carboxypeptidase: Penicillin-sensitive enzymatic reactions, *Fed. Proc. 26*, 9−22.
5. Adams, E. (1976) Catalytic Aspects of Enzymatic Racemization, in *Advances in Enzymology* (Meister, A., Ed.) pp 69−138, John Wiley & Sons, New York.
6. Martinez-Carrion, M., and Jenkins, W. T. (1965) D-Alanine-D-glutamate transaminase. I. Purification and characterization, *J. Biol. Chem. 240*, 3538−3546.
7. Sun, S., and Toney, M. D. (1999) Evidence for a two-base mechanism involving tyrosine-265 from arginine-219 mutants of alanine racemase, *Biochemistry 38*, 4058−4065.
8. Stamper, G. F., Morollo, A. A., Ringe, D., and Stamper, C. G. (1998) Reaction of alanine racemase with 1-aminoethylphosphonic acid forms a stable external aldimine, *Biochemistry 37*, 10438−10445.
9. Watanabe, A., Kurokawa, Y., Yoshimura, T., and Esaki, N. (1999) Role of tyrosine 265 of alanine racemase from *Bacillus stearothermophilus*, *J. Biochem. 125*, 987−990.
10. Spies, M. A., and Toney, M. D. (2003) Multiple Hydrogen Kinetic Isotope Effects for Enzymes Catalyzing Exchange with Solvent: Application to Alanine Racemase, *Biochemistry 42*, 5099−5107.
11. Shaw, J. P., Petsko, G. A., and Ringe, D. (1997) Determination of the structure of alanine racemase from *Bacillus stearothermophilus* at 1.9 Å resolution, *Biochemistry 36*, 1329−1342.
12. Watanabe, A., Yoshimura, T., Mikami, B., Hayashi, H., Kagamiyama, H., and Esaki, N. (2002) Reaction mechanism of alanine racemase from *Bacillus stearothermophilus*: X-ray crystallographic studies of the enzyme bound with N-(5′-phosphopyridoxyl)alanine, *J. Biol. Chem. 277*, 19166−19172.
13. Morollo, A. A., Petsko, G. A., and Ringe, D. (1999) Structure of a Michaelis complex analogue: Propionate binds in the substrate carboxylate site of alanine racemase, *Biochemistry 38*, 3293−3301.
14. Ondrechen, M. J., Briggs, J. M., and McCammon, J. A. (2001) A model for enzyme−substrate interaction in alanine racemase, *J. Am. Chem. Soc. 123*, 2830−2834.
15. Peisach, D., Chipman, D. M., Van Ophem, P. W., Manning, J. M., and Ringe, D. (1998) D-Cycloserine inactivation of D-amino acid aminotransferase leads to a stable noncovalent protein complex with an aromatic cycloserine-PLP derivative, *J. Am. Chem. Soc. 120*, 2268−2274.
16. Fenn, T. D., Stamper, G. F., Morollo, A. A., and Ringe, D. (2003) A Side Reaction of Alanine Racemase: Transamination of Cycloserine, *Biochemistry 42*, 5775−5783.
17. Olson, G. T., Fu, M., Lau, S., Rinehart, K. L., and Silverman, R. B. (1998) An aromitization mechanism of inactivation of γ-aminobutyric acid aminotransferase for the antibiotic L-cycloserine, *J. Am. Chem. Soc. 120*, 2256−22267.
18. Noland, B. W., Newman, J. M., Hendle, J., Badger, J., Christopher, J. A., Tresser, J., Buchanan, M. D., Wright, T. A., Rutter, M. E., Sanderson, W. E., Muller-Dieckmann, H. J., Gajiwala, K. S., and Buchanan, S. G. (2002) Structural studies of *Salmonella typhimurium* ArnB (PmrH) aminotransferase: A 4-amino-4-deoxy-L-arabinose lipopolysaccharide-modifying enzyme, *Structure 10*, 1569−1580.
19. Malashkevich, V. N., Strop, P., Keller, J. W., Jansonius, J. N., and Toney, M. D. (1999) Crystal structures of dialkylglycine decarboxylase inhibitor complexes, *J. Mol. Biol. 294*, 193−200.
20. Miles, E. W. (1985) Transamination as a Side Reaction of Other Phosphopyridoxal Enzymes, in *Transaminases* (Christen, P., and Metzler, D. E., Eds.) pp 470−500, John Wiley & Sons, New York.
21. Cook, S. P., Galve-Roperh, I., Martinez del Pozo, A., and Rodriguez-Crespo, I. (2002) Direct calcium binding results in activation of brain serine racemase, *J. Biol. Chem. 277*, 27782−27792.
22. Kurokawa, Y., Watanabe, A., Yoshimura, T., Esaki, N., and Soda, K. (1998) Transamination as a side-reaction catalyzed by alanine racemase of *Bacillus stearothermophilus*, *J. Biochem. 124*, 1163−1169.
23. Neidhart, D. J., Distefano, M. D., Tanizawa, K., Soda, K., Walsh, C. T., and Petsko, G. A. (1987) X-ray crystallographic studies of the alanine-specific racemase from *Bacillus stearothermophilus*. Overproduction, crystallization, and preliminary characterization, *J. Biol. Chem. 262*, 15323−15326.
24. Otwinowski, Z., and Minor, W. (1997) in *Methods in Enzymology* (Carter, C. W., and Sweet, R. M., Eds.) pp 307−326, Academic Press, New York.
25. Brunger, A. T. (1992) The free *R* value: A novel statistical quantity for assessing the accuracy of crystal structures, *Nature 355*, 472−474.
26. Brunger, A. T., Adams, P. D., Clore, G. M., DeLano, W. L., Gros, P., Grosse-Kunstleve, R. W., Jiang, J. S., Kuszewski, J., Nilges, M., Pannu, N. S., Read, R. J., Rice, L. M., Simonson, T., and Warren, G. L. (1998) Crystallography & NMR system: A new software suite for macromolecular structure determination, *Acta Crystallogr. D54* (Part 5), 905−921.
27. Read, R. J. (1986) Improved Fourier coefficients for maps using phases from partial structures with errors, *Acta Crystallogr. A42*, 140−149.
28. Jones, T. A., Zou, J. Y., Cowan, S. W., and Kjeldgaard, M. (1991) Improved methods for building protein models in electron density maps and the location of errors in these models, *Acta Crystallogr. A47* (Part 2), 110−119.
29. Wang, E., and Walsh, C. (1978) Suicide substrates for the alanine racemase of *Escherichia coli* B, *Biochemistry 17*, 1313−1321.
30. Watanabe, A., Kurokawa, Y., Yoshimura, T., and Esaki, N. (1999) Role of tyrosine 265 of alanine racemase from *Bacillus stearothermophilus*, *J.f Biochem. 125*, 987−990.
31. Laskowski, R. A., Moss, D. S., and Thornton, J. M. (1993) Main-chain bond lengths and bond angles in protein structures, *J. Mol. Biol. 231*, 1049−1067.

32. Kallen, R. G., Korpela, T., Martell, A. E., Matsushima, Y., Metzler, C. M., Metzler, D. E., Morozov, Y. V., Ralston, I. M., Savin, F. A., Torchinsky, Y. M., and Ueno, H. (1985) Chemical and Spectroscopic Properties of Pyridoxal and Pyridoxamine Phosphates, in *Transaminases* (Christen, P., and Metzler, D. E., Eds.) pp 38−108, John Wiley & Sons, New York.
33. Faraci, W. S., and Walsh, C. T. (1988) Racemization of alanine by the alanine racemases from *Salmonella typhimurium* and *Bacillus stearothermophilus*: Energetic reaction profiles, *Biochemistry 27*, 3267−3276.
34. Taoka, S., and Banerjee, R. (2002) Stopped-flow kinetic analysis of the reaction catalyzed by the full-length yeast cystathionine β-synthase, *J. Biol. Chem. 277*, 22421−22425.
35. Sivaraman, J., Li, Y., Larocque, R., Schrag, J. D., Cygler, M., and Matte, A. (2001) Crystal structure of histidinol phosphate aminotransferase (HisC) from *Escherichia coli*, and its covalent complex with pyridoxal-5′-phosphate and l-histidinol phosphate, *J. Mol. Biol. 311*, 761−776.
36. Spies, M. A., Woodward, J. J., Watnik, M. R., and Toney, M. D. (2004) Alanine racemase free energy profiles from global analyses of progress curves, *J. Am. Chem. Soc. 126*, 7464−7475.
37. Braunstein, A. E. (1973) Amino Group Transfer, in *The Enzymes* (Boyer, P. D., Ed.) pp 379−481, Academic Press, New York.
38. Fenn, T. D., Ringe, D., and Petsko, G. A. (2003) POVScript+: A program for model and data visualization using persistence of vision raytracing, *J. Appl. Crystallogr. 36*, 944−947.
39. Tanner, M. E. (2002) Understanding Nature's Strategies for Enzyme-Catalyzed Racemization and Epimerization, *Acc. Chem. Res. 35*, 237−246.
40. Thornberry, N. A., Bull, H. G., Taub, D., Wilson, K. E., Guillermo, G. G., Rosegay, A., Soderman, D. D., and Patchett, A. A. (1991) Mechanism-based Inactivation of Alanine Racemase by 3-Halovinylglycines, *J. Biol. Chem. 266*, 21657−21665.

BI047842L